

# **ADVANCED DIE MATERIALS AND LUBRICATION SYSTEMS TO REDUCE DIE WEAR IN HOT AND WARM FORGING**

**Dr. Taylan Altan, Professor and Director, and Mr. Manas Shirgaokar, Graduate  
Research Associate**

**ERC for Net Shape Manufacturing, the Ohio State University,  
339 Baker Systems, 1971 Neil Ave, Columbus OH 43210 USA**

[www.ercnsm.org](http://www.ercnsm.org)

## **ABSTRACT**

Hot and warm forging processes subject the dies to severe cyclic thermal and mechanical fatigue subsequently resulting in die failure primarily through wear, plastic deformation and heat checking. This ongoing study aims to reduce die wear through application of proprietary hot-work tool steels and ceramic-based materials through combination of computational analysis and shop floor experimentation. As part of this initiative guidelines will be developed for a) die design under hot and warm forging conditions, and b) selection of optimum lubrication systems for increased die life. The goals of this FIERF-sponsored study will be achieved through active cooperation with a number of FIA member companies involved in forging, lubrication and tooling.

## **1 INTRODUCTION**

Die costs can constitute up to 30% of the production cost of a part and also affect its profitability directly (die manufacturing cost) and indirectly (repair, press downtime, scrap, rework etc). Hot and warm forging processes subject the dies to severe thermal and mechanical fatigue due to high pressure and heat transfer between the dies and the workpiece. High cyclic surface temperatures result in thermal softening of the surface layers of the dies, subsequently increasing die wear and susceptibility to heat checking.

Conventional methodologies such as nitriding or boriding result in a significant increase in die surface hardness but have not resulted in substantial improvements in die service life. Recently, a number of advanced grades of proprietary hot-work tool steels have been introduced targeted specifically for warm and hot forging applications. Additionally, the potential for use of ceramic and carbide-based materials in appropriate applications is also of interest.

This study proposes to investigate the application of these advanced die materials along with the optimum lubrication system for substantial improvement of die service life in hot and warm forging. It is also emphasized that die design improvements need to be implemented along with the use of advanced die materials in order to realize their maximum potential. This is demonstrated here through some research and production case studies from this project and overseas (Germany and Japan).

## **2 OBJECTIVES AND APPROACH**

This study officially started on July 15, 2006 with a proposed duration of 12 months and the overall goal of developing techniques to predict and improve die life in hot and warm forging. The following objectives were outlined when the study commenced:

- a) Improvement of die life in warm and hot forging through application of advanced die materials.
- b) Development of guidelines for selecting the optimum (cost/productivity) die material and lubrication system for a given application.

The goals of this study will be achieved through computational analysis using the commercial finite element simulation code DEFORM™ and subsequent validation with forging trials in cooperation with participating companies.

## **3 CURRENT STATUS**

The following is a brief summary of the current project status:

- A project website has been created in order to provide up-to-date access to all project documentation to the participating companies. This information can be accessed through the official website of the Center for Precision Forming (formerly Engineering Research Center for Net Shape Manufacturing) at [www.ercnsm.org](http://www.ercnsm.org).
- Detailed questionnaires were prepared and sent to a) the participating forging companies in order to gather process and die wear related information, and b) the tooling companies to collect die material properties.
- A project kick-off meeting was organized on September 28, 2006 at The Ohio State University in Columbus, OH. The purpose of this meeting was to outline the scope of the study and identify common die wear related issues. A few potential parts and die materials were selected for future analysis and trials.
- FE analysis was conducted for a few selected parts. A hot forged component was selected in cooperation with Impact Forge (Columbus, IN) for initial analysis and production trials. Die design changes were suggested to reduce contact time with the heated part in critical regions of the dies. Forging trials with advanced hot-work tool steels have been planned tentatively for March 2007.

## **4 LITERATURE REVIEW OF DIE WEAR STUDIES**

An important part of the current research study is to review the global hot and warm forging technology with an emphasis on die wear related studies. Two literature reports have so far been provided covering research work conducted in some German institutes along with production case studies from Japan using ceramic/cermet die materials. Development of some proprietary hot-work tool steel grades for warm and hot forging was also covered along with production case studies. Some of these examples are briefly mentioned in the following sections.

### 4.1.1 Case Studies from Germany

The examples provided in this section relied on extensive university-based experiments conducted under practical hot forging conditions. Different coating systems and joining techniques for ceramic inserts were investigated for axisymmetric parts and precision forged gears. This information was obtained from the following two sources through contacts established by the CPF (ERC/NSM):

- Institute of Metal Forming and Metal Forming Machine Tools (IFUM), University of Hannover.
- Chair of Manufacturing Technology, University of Erlangen.

Multi-layer duplex coatings and ceramic inserts (SiAlON and silicon nitride) were applied to hot forging of helical spur gears. The 18 layer duplex system showed superior wear reduction over 1000 and 2000 forging cycles (Figure 1). The coatings were applied according to their final achievable hardness in order to give a smooth transition from the coating with maximum hardness (TiC) to that with the lowest hardness (TiN).

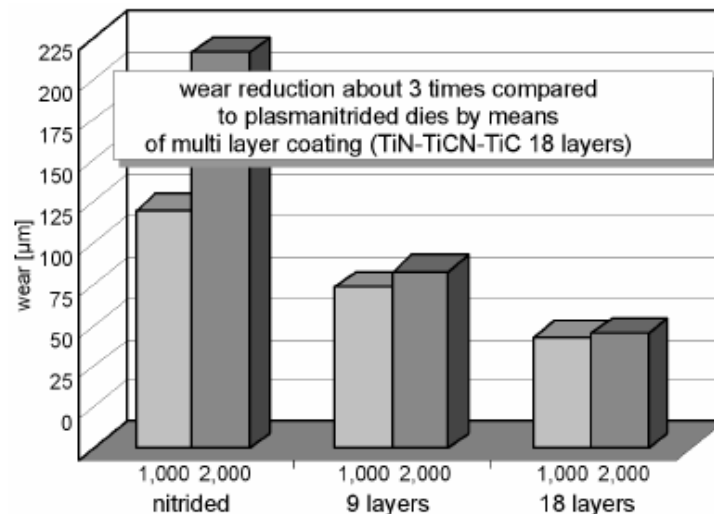
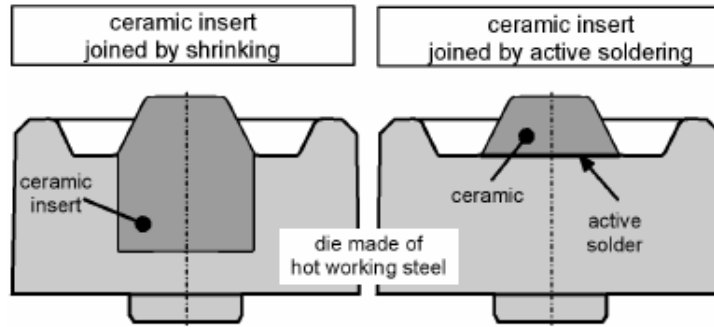


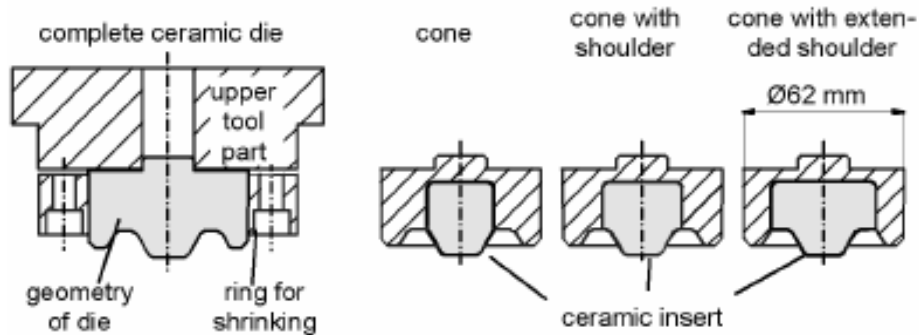
**Figure 1: Performance of ceramic multi-layer coatings compared to nitrided hot-work tool steel (1).**

For investigations with ceramic inserts, two assembly techniques were explored as shown in Figure 2a. Of these two techniques, brazing is more flexible since it allows the application of inserts in complex tool geometries in wear critical areas. One of the drawbacks of this method, however, is the residual stresses generated from brazing. Thermal shrinking on the other hand is better suited for axisymmetric geometries. The different insert geometries investigated are shown in Figure 2b. The effect of different interference fits and preheat temperatures was not investigated in these studies.

Figure 3 shows the wear performance for the ceramic dies compared to nitrided hot-work tool steel for two different forging (workpiece) temperatures after 500 forging cycles. Silicon nitride showed superior wear resistance (3 to 6 times less wear) among the die materials selected.



a) Two types of insert design investigated viz. shrink-fit and brazed.



b) Different types of shrink-fit designs investigated in forging trials.

Figure 2: Die designs investigated in forging trials with ceramic inserts (1).

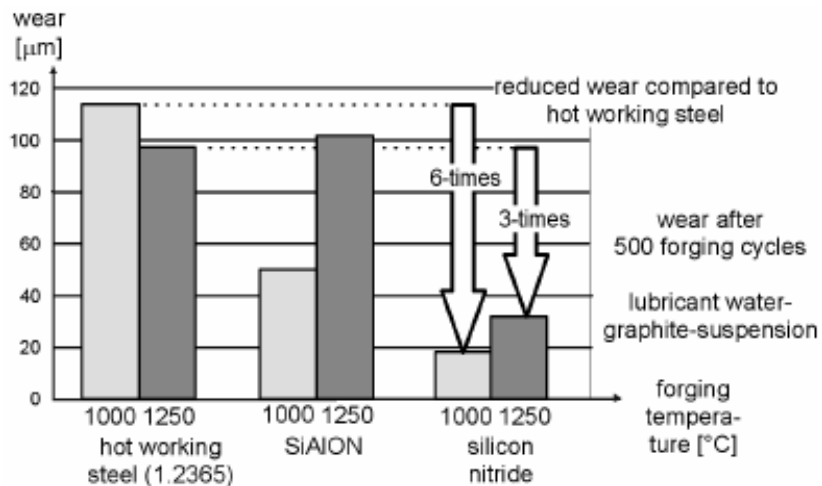
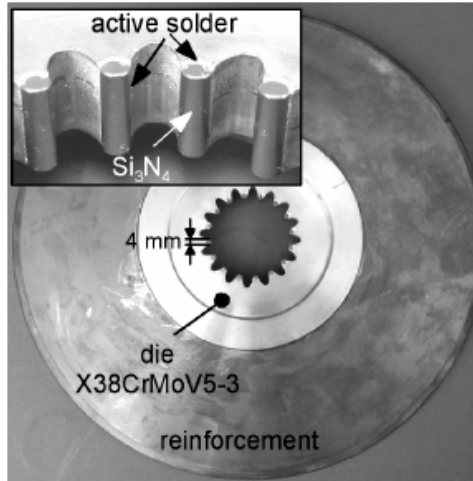


Figure 3: Performance of ceramic die materials in forging trials (1).

It was observed during the trials with active brazed inserts that solder quality has to be controlled consistently in order to prevent premature failure of the die in service. A hot forging die with 16 inserts was being considered for precision forging of spur gears (Figure 4). Results from these trials are not currently available.



**Figure 4: Die with ceramic inserts for precision hot forging of spur gears (1).**

#### 4.1.2 Case Studies from Japan

There have been cases of successful production application of cermet/ceramic dies in Japan. These publications were in Japanese and only provided limited information. Nissan Motor Co. is using cermet dies made of MoB (ceramic). The material is powder formed and sintered. In production tests, two die materials were tested on forward extrusion of outer race part under warm forging conditions (Figure 5), namely, a) nickel-based superalloy, and b) MoB cermet.

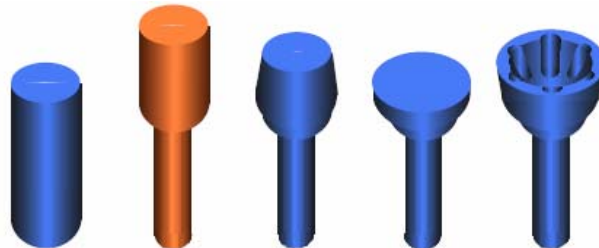
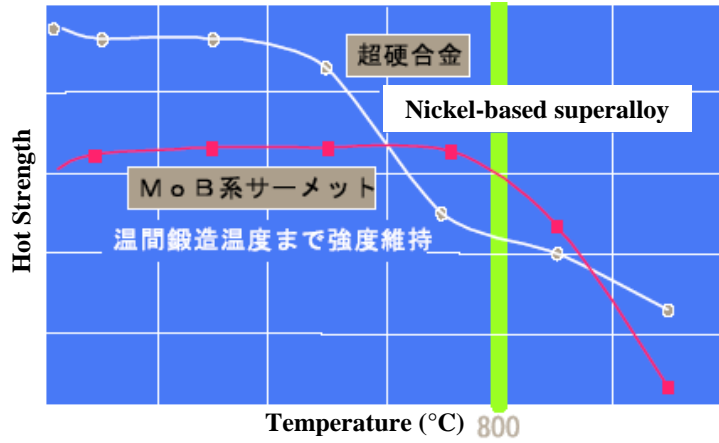


**Figure 5: Forward extrusion of outer race part (2).**

Figure 6 shows the high temperature strength of the two die materials. Though the axes are not labeled, it can clearly be seen that MoB cermet die can withstand higher temperature (800°C/1470°F) than the superalloy. Figure 6b also shows die seizure observed with the superalloy material.

Figure 7 shows two shrink-fitted hot forging die design examples using ceramic and cermet die inserts with shrink-rings made of hot-work tool steel. Both die designs were implemented in production and involved in-depth experimental analyses of the effect of preheat and forging temperatures on the interference fits at the shrink ring interfaces. It was found that the thermal expansion from preheating and forging had a significant measurable effect on the pre-stress from shrink-fitting. For the Ti alloy preforms, an 82% reduction in shrink-fit was observed after preheating to a temperature of 540°C (1000°F) with just the inner shrink ring (5 in Figure 7a). With the outer shrink ring

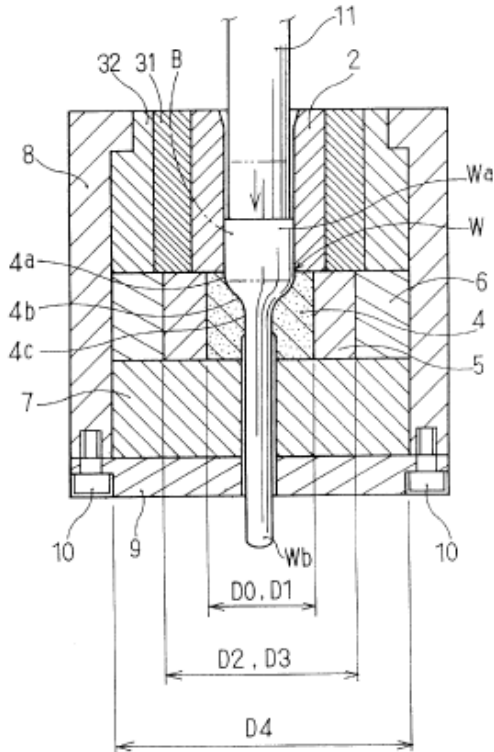
installed a 47% reduction was observed (3). These examples demonstrate that the use of room temperature dimensions and shrink-fit values for analysis of hot and warm forging tooling can lead to incorrect judgments.



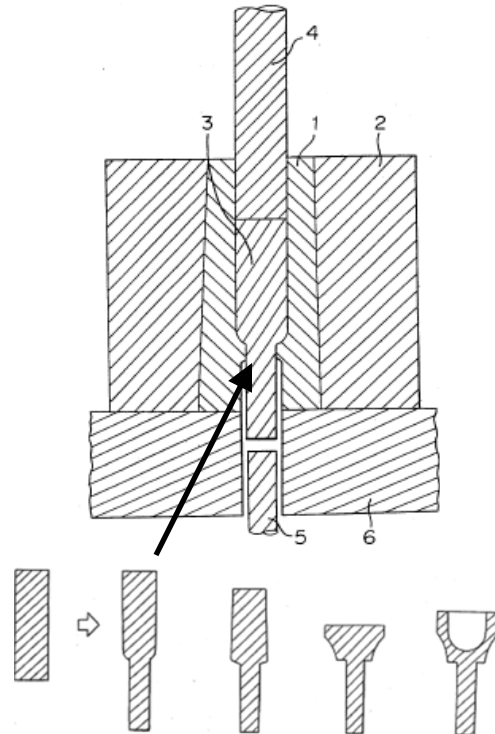
(a)

(b)

Figure 6: Forging tests with superalloy and cermet materials. a) Influence of warm forging temperature on the strength of die material, b) Dies seizure when super alloy dies were used (2).



a) Ti alloy valve preforms (3).



b) Hot forging (4).

Figure 7: Shrink-fit die designs for hot forging with ceramic and cermet inserts.

## 5 RESULTS FROM THE FIERF DIE WEAR STUDY

### 5.1 Example Parts and Die Materials Selected for the Study

Following the kick-off meeting organized at the start of the project, it was decided to first analyze simple axisymmetric geometries before experimenting with the more complex parts. Table 1 shows the example geometries selected for the study. The die materials being considered in this study can be categorized as follows:

- Proprietary grades of advanced hot-work tool steels recently introduced or under development specifically for warm and hot forging process conditions. e.g. W360™ from Böhler-Uddeholm ([www.bucorp.com](http://www.bucorp.com)), Thyrotherm 2999 EFS-SUPRA™ from Schmolz+Bickenbach ([www.schmolz-bickenbach.com](http://www.schmolz-bickenbach.com)).
- Matrix high speed tool steels e.g. MDS™ series available from Nachi-Fujikoshi/Walter Metals ([www.waltermetals.com](http://www.waltermetals.com)), DRM™ series from Daido Steel ([www.daidosteel.com](http://www.daidosteel.com)).
- Coated and uncoated ceramic-based materials e.g. Silicon Aluminum Oxynitride (SiAlON), silicon nitride, etc. from Kennametal ([www.kennametal.com](http://www.kennametal.com)).

**Table 1: Example production parts with die wear problems.**

Name	Description	Failure mechanism
Reverse piston	Axisymmetric disc shaped part with upsetting and extrusion on a mechanical press.	Wear and thermal fatigue.
Turbine shaft	Axisymmetric shaft with upsetting operation on a hydraulic press.	Thermal fatigue.
Gear blank	Axisymmetric part with upsetting operation on a Hatebur™.	Wear
Actuator forging	Asymmetric shaft with upsetting operation on a mechanical press.	Wear
Control arm	Asymmetric part forged on a mechanical press.	Wear

Figure 8 shows some of these die materials compared to a generic hot-work tool steel (H-13) in terms of hot hardness. Die materials will be selected for a given process based upon a) the interface conditions (temperatures, loading conditions, etc.) determined through FEA, and b) comparison of the material properties (mechanical and thermal) of the tool steels or ceramics.

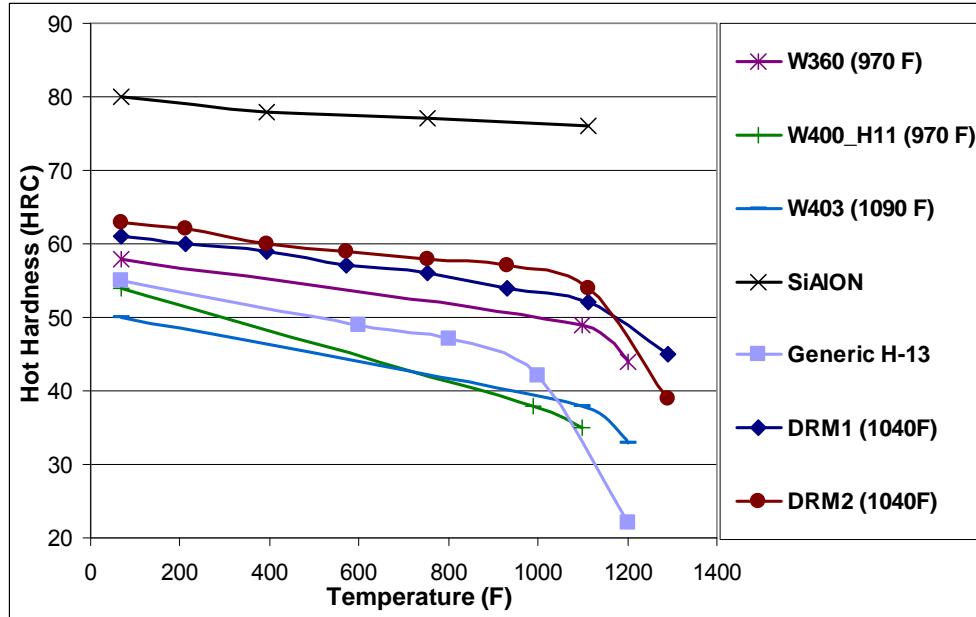


**Figure 8: Advanced hot-work tool steel grades compared with a generic H-13 grade and a ceramic die material (SiAlON) on the basis of hot hardness.**

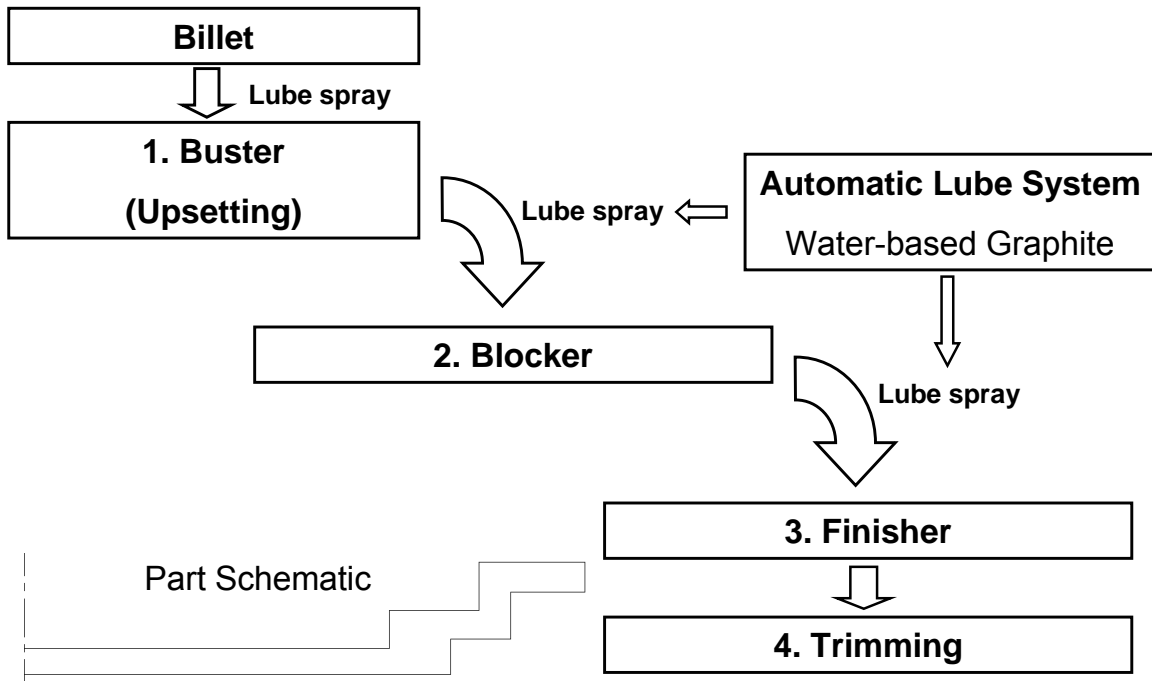
## 5.2 FIERF Case Study 1: Hot Forging of a Reverse Piston

Figure 9 shows the hot forging sequence for the reverse piston. The dominant failure mechanism in the current forging process is thermal fatigue. The general process description is provided below with details sanitized in order to maintain confidentiality:

- A steel billet is induction heated to the hot forging temperature of  $\approx 1150^{\circ}\text{C}$  ( $2100^{\circ}\text{F}$ ) and forged to the final shape in three sequential steps in a mechanical press. The initial buster operation generates a pancake shape. Part transfer is done manually.
- The dies (hot-work tool steel) are preheated to  $\approx 150^{\circ}\text{C}$  ( $300^{\circ}\text{F}$ ) and cooled with an automatic lubrication system (water-based graphite).

Most automotive parts have stringent requirements on surface finish. After the onset of thermal fatigue, the heat checking pattern is imprinted onto the part surface. Thus, the part meets dimensional requirements but not those on the surface finish. Since the bottom die is in contact with the workpiece longer than the top die it is subjected to greater thermal loads and has a shorter lifespan. Thus, the die change is dictated by the life of the bottom blocker die.





**Figure 9: Schematic of the hot forging process sequence for the example part.**

### 5.2.1 FE Simulation of the Current Process

Information from the process and die material questionnaires was used as input to the commercial FEM code DEFORM™ in order to determine the die-workpiece interface conditions for the current process set-up. For preliminary simulations the initial die temperature was assumed as uniform, based upon the specified pre-heat temperature. Also, the die material was assumed as homogeneous i.e. the effect of surface treatment was neglected.

The FE simulation strategy to determine the interface conditions for the selected part is explained by first considering a single forging cycle ( $t_f - t_0$ ) in a mechanical press (Figure 10):

- I. Part Loading ( $t_a - t_0$ ).
- II. Clutch Activation ( $t_b - t_a$ ).
- III. Forging Stroke ( $t_c - t_b$ ); neglecting elastic deflection at bottom dead center (BDC).
  - Average contact time for top die/punch ( $t_2 - t_1$ ) i.e. actual forging process.
  - Average contact time for bottom die ( $t_c - t_0$ ).
- IV. Knockout ( $t_d - t_c$ ).
- V. Part Transfer/Removal ( $t_e - t_d$ ).
- VI. Lube Spray ( $t_f - t_e$ ).

Of the six stages shown in Figure 11, stages III to VI (forging, part removal and cooling) were considered for the selected part using DEFORM™.

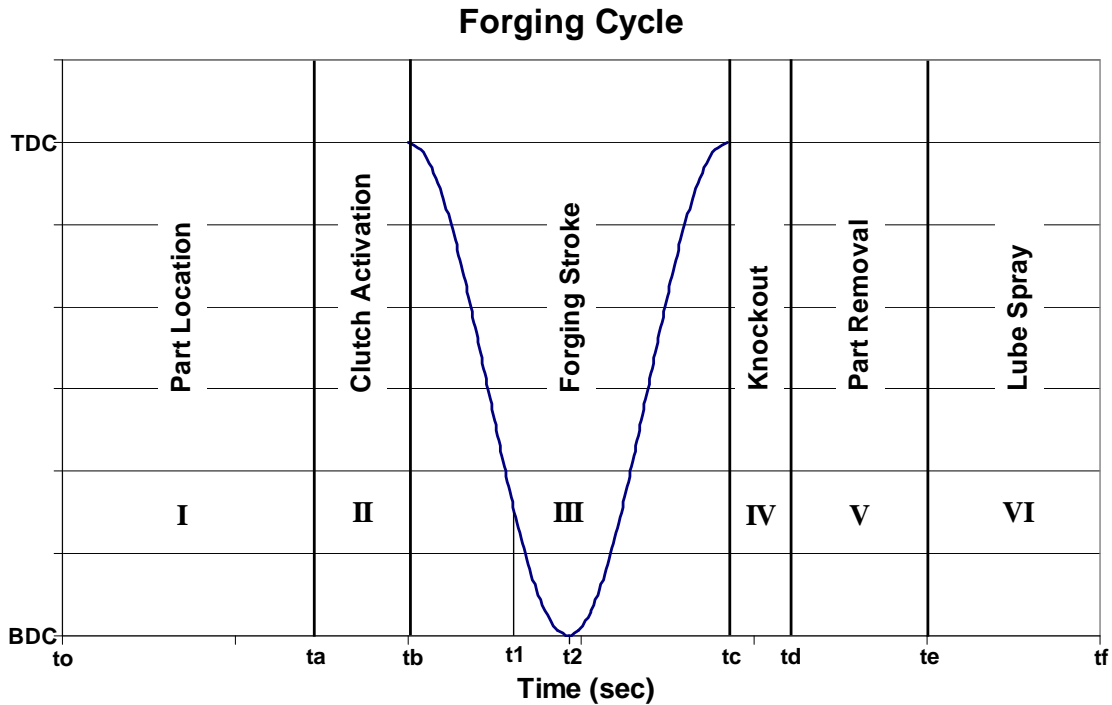


**Figure 10: Description of a single forging cycle on a mechanical press.**

Figure 11 shows an example hot forging temperature cycle for the dies on a mechanical press. The complete forging cycle was simulated starting with the ram at top dead center (TDC) and with the die at a uniform preheat temperature ( $T_0$ ) (Figure 11). Thus, die chilling as well as dwell time before knockout were taken into consideration. During “die chill”, the heated billet or preform was on the lower die. After “forging”, the forged part remains on the lower die during the “dwell” period. After the forging is removed, both, upper and lower dies are sprayed with the lubricant during the “cooling” period. The temperature drop during cooling is shown approximated as linear. This stage was simulated by exposing the die surface to an assumed lubricant temperature for a specific time with a convective heat transfer coefficient obtained from literature on spray tests. The die surface temperature drops rapidly during lubricant spray but increases again in the dwell time during part transfer from the previous forging station (part of the cooling phase in Figure 11). This process was simulated by using a lower value of the heat transfer coefficient (corresponding to air) to emulate heat transfer with ambient temperature in the forging environment. Simulations can be calibrated later based on production die temperature and transfer time measurements obtained during forging trials.

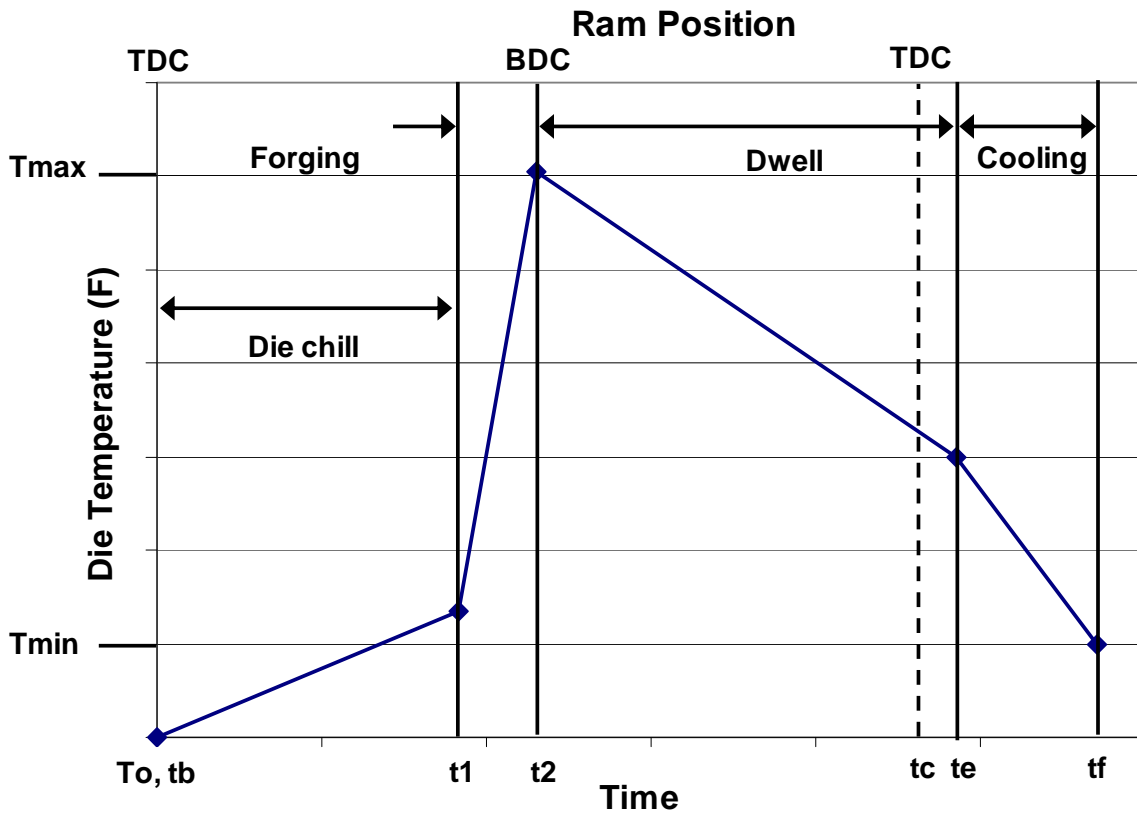


Figure 11: Die temperature cycle for a typical forging process in a mechanical press.

### 5.2.2 Die Temperatures during Steady-State

Accurate die design (stress analysis) and prediction of die wear in hot and warm forging also requires investigation of the production process under steady-state conditions. All forming processes, especially warm/hot forging, have a transient warm-up period before the dies reach their steady operating temperature distribution. Most FE simulation-based analyses ignore this warm-up stage by assuming a uniform pre-heat temperature for the dies, which is acceptable for metal flow analysis.

Figure 12 shows a schematic representation of the warm-up phase of hot forging dies with an initial preheat temperature of  $T_0$ . The average die temperature before the start of the forging stroke ( $T_i$ ) increases until a steady-state cycle is reached ( $T_{min}$ ). As shown in Figure 12, the starting die temperature ( $T_i$ ) for an arbitrary forging cycle prior to reaching steady-state can be expressed as the summation of the starting temperature ( $T_0$ ; ambient or preheat) and the temperature increase from each of the previous forging cycles ( $\delta T$ ):

$$T_i = \delta T_{i-1} + \delta T_{i-2} + \delta T_{i-3} + \dots + T_0 = T_0 + \Delta T \quad \text{Equation – 1}$$

This increase in die temperature will be monitored during production in order to determine the average temperature increase of the die surface layers as a function of forging cycles for a given production process.

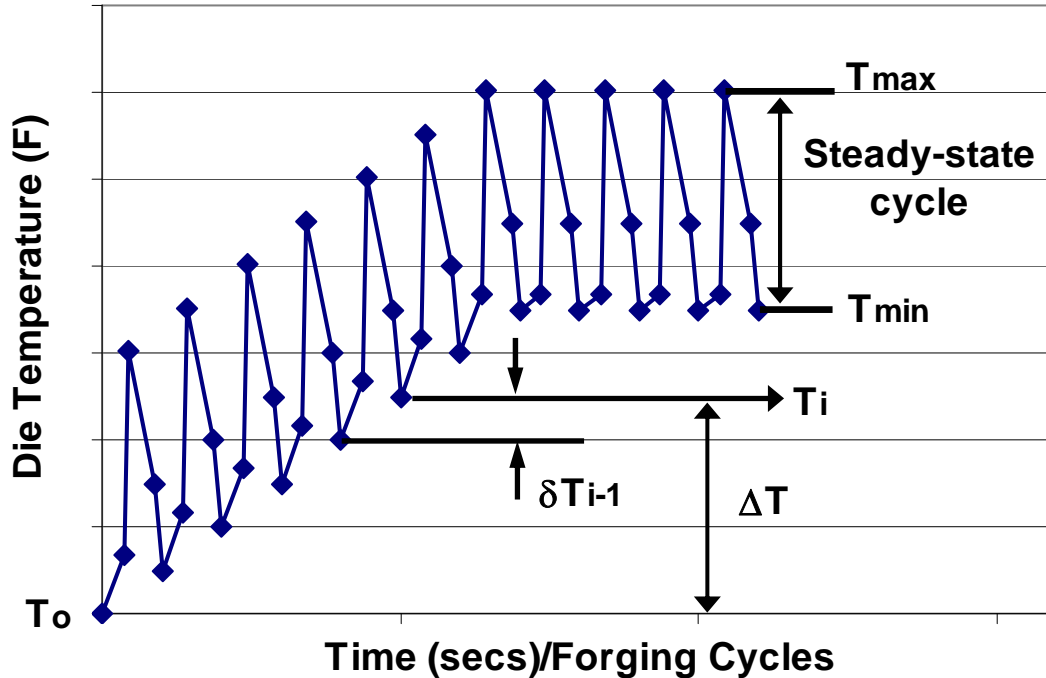


**Figure 12: Schematic representation of warm-up in forging dies.**

Thus, the FE analysis sequence is summarized as follows:

- Step 1: Simulate the entire ram stroke considering heat-transfer between the dies and the workpiece.
- Step 2: Simulate the cooling stage in two steps viz. a) lubricant spray and b) dwell time till next forging stroke.

The above sequence provides the temperature distribution in the die after one forging cycle. The knockout and part removal stages were not simulated but can be easily accounted for later when detailed cycle time information is available.

### 5.2.3 Analysis of Die-Workpiece Interface Conditions

The W360™ die material was selected for comparison with H-13 because of its high thermal conductivity and hot hardness (Figure 8). For the die-workpiece contact times of the current process, the performance of the two die materials was compared virtually on the basis of predicted temperature distributions after forging and cooling. Though FE analysis was conducted for all three forging steps shown in Figure 9, results are presented only for the blocker stage, which was the one with the most severe thermal fatigue problem.

#### 5.2.3.1 Temperature Distribution after Forging

For the current die design and mechanical press behavior, the following observations were recorded in the FE simulation with regard to the contact time between the blocker dies (top and bottom) and workpiece:

- The top die was in contact with the workpiece for  $\approx 40 - 80$  milliseconds depending upon the region of interest.
- Certain local regions of the bottom die have significantly higher contact times (0.46 - 0.92 seconds) compared to the top die e.g. region where preform rests on the bottom die.

Areas with higher contact times were more susceptible to thermal fatigue due to their higher temperatures. The following observations were recorded regarding the die temperature distribution:

- At BDC (time  $t_2$  in Figure 11): With a preheat temperature of  $\approx 150^\circ\text{C}$  ( $300^\circ\text{F}$ ), the H-13 and W360™ dies showed maximum local temperatures of  $\approx 460^\circ\text{C}$  ( $860^\circ\text{F}$ ) and  $415^\circ\text{C}$  ( $780^\circ\text{F}$ ), respectively at the end of deformation (ram at BDC). Overall, the 25-30% higher thermal conductivity of W360™ resulted in  $\approx 10-15\%$  lower temperatures in the surface layers, since heat is conducted away more rapidly. The die temperatures were localized in the upper 1 to 2.5 mm (0.04 to 0.1 inches) of the die surface at BDC.
- At TDC (time  $t_c$  in Figure 11): At the end of the forging cycle (ram at TDC), the die surface temperatures ranged between  $190$  to  $230^\circ\text{C}$  ( $370$  to  $475^\circ\text{F}$ ), with the surface temperatures in the W360™ die being  $\approx 6-7\%$  lower. The temperature increase at this stage of the process was localized in the upper 5 to 7.5 mm (0.2 to 0.3 inches) of the die surface. This temperature distribution was carried forward into the simulation of the lubricant spray.

Based on the above observations, it was concluded that in addition to changing die materials, design changes were required in the buster or blocker die to ensure that contact times were reduced in the functional regions of the die i.e. those that form the final part.

### 5.2.3.2 Temperature Distribution after Cooling

Cooling was simulated in the following two steps, assuming a duration of 0.2 seconds each:

- Lube spray: A uniform constant heat transfer coefficient of  $35 \text{ kW/m}^2\text{-K}$  ( $6164 \text{ Btu/hr-ft}^2\text{-F}$ ) was applied (assuming lube temperature of  $20^\circ\text{C}/68^\circ\text{F}$ ).
- Dwell time: Assuming ambient temperature of  $20^\circ\text{C}$  ( $68^\circ\text{F}$ ), a heat transfer coefficient of  $4 \text{ kW/m}^2\text{-K}$  ( $0.0227 \text{ Btu/hr-ft}^2\text{-F}$ ) was applied on the die surface.

Average surface temperatures in the die cavity ranged between  $120$  to  $150^\circ\text{C}$  ( $250$  to  $300^\circ\text{F}$ ) prior to the next forging stroke. The FE predictions will be compared with data gathered from production in order to calibrate the spray time and heat transfer boundary conditions. Using the current FE model it is possible to generate temperature profiles for different heat transfer coefficients and match them to different spray settings.

#### 5.2.4 Improved Process Design for Forging Trials

Based upon the analysis of the die-workpiece interface conditions a two-pronged approach was adopted to improve the die life for the selected process. Along with the application of an advanced die material, the forging process design would be modified in order to reduce the contact time in critical regions of the bottom dies in the blocker and finisher stage. The following is a summary of the proposed forging trials:

- Die Material: An advanced die material (initially W360™) will be used with the recommended heat treatment practice for the first forging trial. No surface treatment will be used initially, but may be added for a second trial.
- Die Design: The buster operation was modified such that the preform does not contact the functional surfaces of the bottom blocker when placed on it. Additionally, the flash region in the finisher will be modified in order to hold the blocker preform above the die surface until the top die contacts it.
- Die Material Characterization: Die coupons will be heat treated with the dies and characterized on the basis of hardness vs. depth before and after forging trials. In the event that a surface treatment is used the effect on hardness and surface roughness will be investigated.

The first forging trials are tentatively scheduled for March 16, 2007.

#### 5.3 FIERF Case Study 2: Shrink-fit Die Design in Hot and Warm Forging

Warm and hot forging processes with geometries that generate high forming pressures and stress concentration require the use of shrink-fit die designs. This is especially true when a ceramic-based die material or one with high hot hardness is used. Current die design and analysis practices apply simplifying assumptions by neglecting the thermal expansion and subsequent change in shrink-fit dimensions (and pre-stress) during die preheating and forging. This case study outlines a procedure to account for the stress and elastic deformation history of a shrink-fit die from room temperature assembly and preheating. A comparison is given between the conventional design analysis and one with the modified procedure outlined here.

A hypothetical warm forging process was considered for demonstrative purposes (Figure 13). A simple forward extrusion process was selected since it is representative of the metal flow occurring during warm/hot forging of automotive components such as exhaust valves, outer races of constant velocity joints, pinions, etc. The process description with the assumptions is as follows:

- A 1045 steel billet ( $\phi$  1.25 inches and length 1.25 inches) is reduced in diameter by 65% in a warm forward extrusion process on a mechanical (eccentric) press.
- A 1600 ton mechanical press was selected from the DEFORM™ equipment database. This press has a stroke of 10 inches and an idle stroking rate of 85 strokes/minute.
- The dies are assumed to be of hot-work tool steel. For the current case the die insert is assumed to be of a proprietary hot-work tool steel (Uddeholm W360™)

and the holder/shrink rings of a generic H13 grade. Some results are also shown for a ceramic insert (SiAlON).

- The billet is induction heated to 815°C (1500°F) and the dies are preheated to 150°C (300°F) prior to the start of production.
- A water-based graphite lubrication/cooling system was assumed for the process with lubricant at room temperature (20°C/68°F).

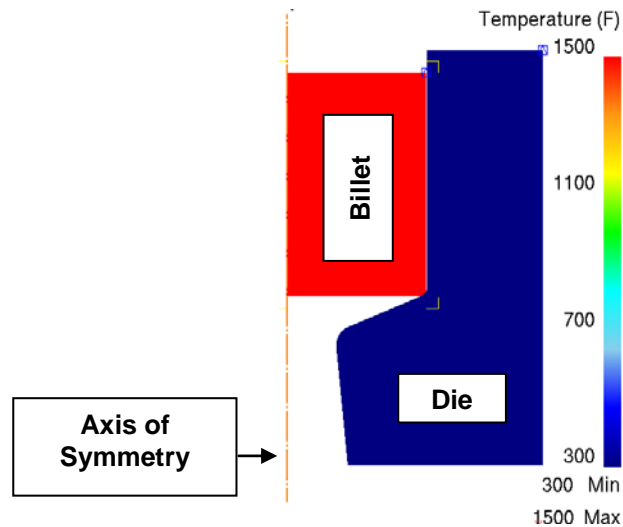


**Figure 13: FE simulation model for the example forward extrusion process.**

Initially a non-isothermal forging simulation was conducted to determine the forging load, temperature distribution and pressure distribution required for die design and stress analysis. The subsequent sections provide an explanation of the procedure used to investigate the effects of the preheat temperature and the forging temperature distribution on the die stress from the shrink fit.

### 5.3.1 Selection of shrink ring dimensions and shrink-fits

Shrink ring dimensions and interference fits are usually selected using equations of infinitely long thick cylindrical shells. A procedure for selecting the appropriate die design for a given internal pressure is provided by various sources (5; 6; 7). For the current case, a die design with two shrink rings was used (Figure 14) for a maximum extrusion pressure estimated at  $\approx 1100$  MPa (160 ksi).

The dies were assumed to be preheated to  $\approx 150^\circ\text{C}$  (300°F) prior to the production run. During steady-state production the die temperature periodically increases (due to heat transfer with the workpiece) and drops (due to the lubricant spray and heat exchange with the environment). The average die temperature for the current design was assumed to be in the 175 to 230°C (350 to 450°F) range based on preliminary simulations. Therefore, the dies were designed using material properties in this temperature range.

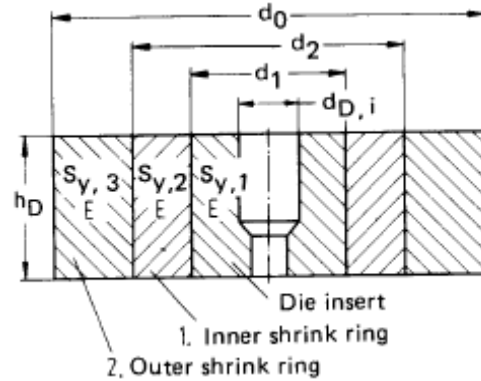


**Figure 14: Schematic representation of die design, with two shrink rings, for forward extrusion (7).**

For the selected temperature range, the tool steel used for the insert (W360™) is assumed to have hardness between 55 to 58 HRC, whereas that for the shrink rings (H13) is assumed to be 45 to 51 HRC (Figure 8), neglecting any tempering effects. Table 2 shows the input values for the calculations with the determined shrink ring dimensions and interference fits shown in Table 3. A factor of safety of roughly 1.25 was used while determining the die dimensions.

**Table 2: Input values used for selection of shrink ring dimensions for the selected temperature range.**

Extrusion pressure	$p_i$	1100 MPa (160 ksi)
Yield strength of insert (W360™)	$S_{y1}$	1585 MPa (230 ksi)
Yield strength of inner ring (H13)	$S_{y2}$	1380 MPa (200 ksi)
Yield strength of outer ring (H13)	$S_{y3}$	1380 MPa (200 ksi)
Inner diameter of the die insert	$d_{D,i}$	32 mm (1.26 in.)
Modulus of elasticity	$E$	190 GPa (27800 ksi)

**Table 3: Interference fit and shrink ring dimensions selected for the assumed process.**

Insert outer diameter	$d_1$	47.676 mm (1.8770 in.)
Inner ring outer diameter	$d_2$	66.606 mm (2.6223 in.)
Outer ring outer diameter	$d_0$	93.048 mm (3.6633 in.)
Diametric Interference at $d_1$	$z_1$	0.1854 mm (0.0073 in.)
Diametric Interference at $d_2$	$z_2$	0.2311 mm (0.0091 in.)



### 5.3.2 Die stresses at room temperature

The pre-stress in the die insert at room temperature due to shrink-fitting was determined by using a one-step die stress analysis. Figure 15 shows the maximum principal stress distribution in the die assembly at room temperature. In the current simulation there is no internal pressure on the die insert. It is therefore a no-load simulation with only the stress distribution from shrink-fitting. After shrink fitting, the insert is under compressive hoop stress whereas the shrink rings are under tensile stress as expected. It should be noted that the die dimensions at the end of this process are different from the design dimensions due to elastic deflection at the shrink-fit interfaces. The simulation model with this elastic stress and deflection history is carried forward to the next analysis step. Ancillary die components, such as backer plates or the holder outside the outer shrink ring were not considered in this analysis.

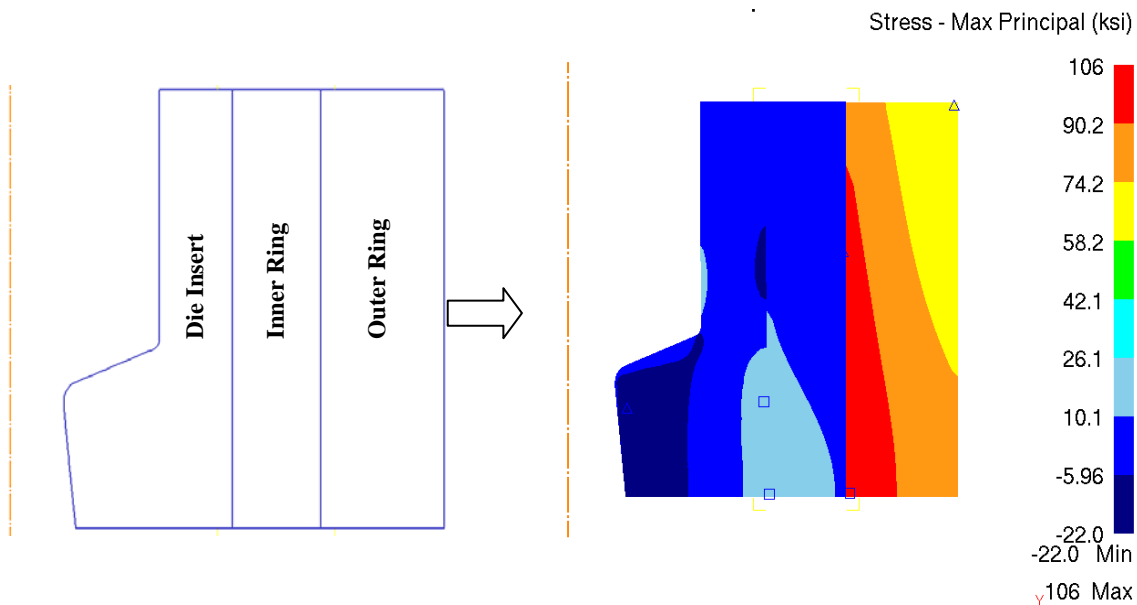


**Figure 15: Maximum principal stress in the two-ring die assembly at room temperature from shrink-fitting.**

### 5.3.3 Die stresses at preheat temperature

For the current process, it is assumed that the dies are heated to a uniform preheat temperature of 150°C (300°F) prior to the start of the forging process. In order to determine the change in the pre-stress (and shrink-fit) with temperature a uniform preheat temperature was assigned to all die components with the stress and elastic deformation history from the room temperature shrink-fit simulation (Section 5.3.2).

The change in the pre-stress from thermal expansion of the die components is shown in Figure 16. The compressive tangential stress in the hot-work tool steel die insert was found to drop by  $\approx 10\%$  due to thermal expansion of the die assembly. For a given die design this drop in pre-stress will increase with the preheat temperature and the difference in thermal expansion coefficients of the two die materials. Significant loss of shrink-fit can occur with inserts made of ceramic-based materials, which can have

thermal expansion coefficients  $\approx$  60-70% lower compared to steel. Figure 17 shows an example case with a ceramic insert that showed a 20% reduction in shrink-fit pressure at the insert-inner ring interface after preheating. It was observed that the inner shrink ring shows a drastic reduction in tensile hoop stress and goes into a primarily compressive state after preheating due to negligible expansion of the insert. Table 4 shows a comparison of the change in shrink-fit interface pressures with the two insert materials after preheating. At present reliable elastic and thermal properties were not available for the ceramic material. Thus, subsequent analysis is shown with the hot-work tool steel insert.

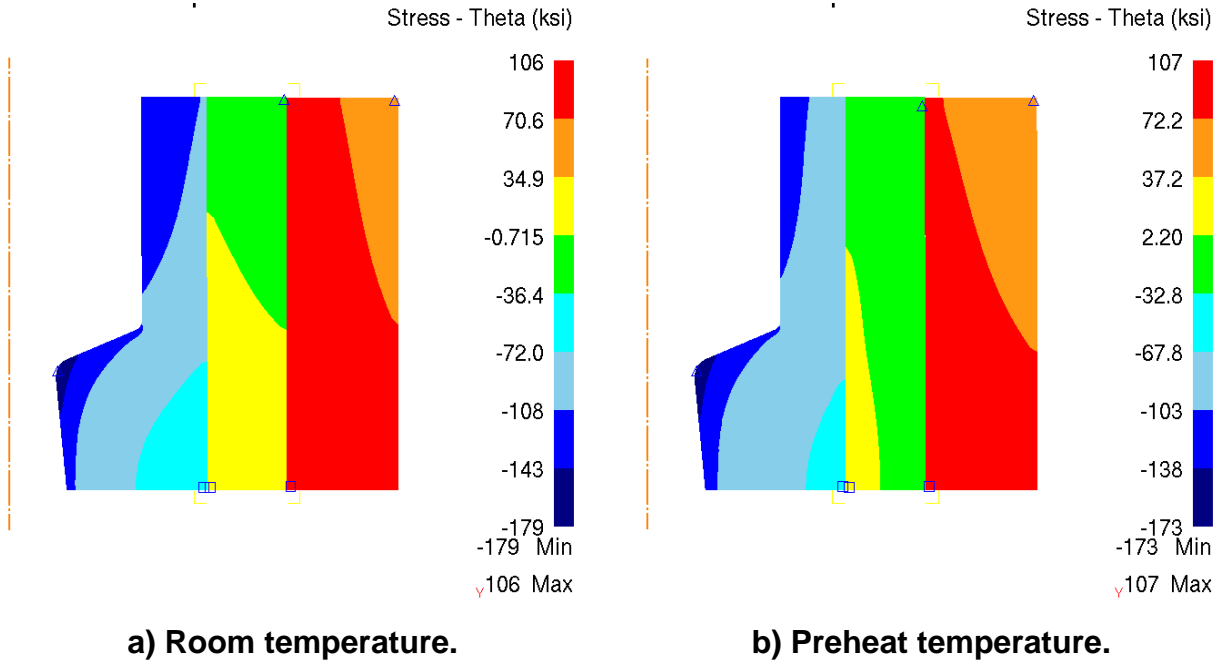


**Figure 16: Change in tangential pre-stress due to preheating for a die assembly with a hot-work tool steel insert.**

**Table 4: Effect of preheat temperature on the interface pressure due to shrink-fitting.**

	Hot-work tool steel (W360™)	Ceramic Insert
Pressure at the insert - inner ring interface	$\approx$ 6% increase	$\approx$ 20% reduction
Pressure at the inner - outer ring interface	$\approx$ 7% increase	$\approx$ 5% increase

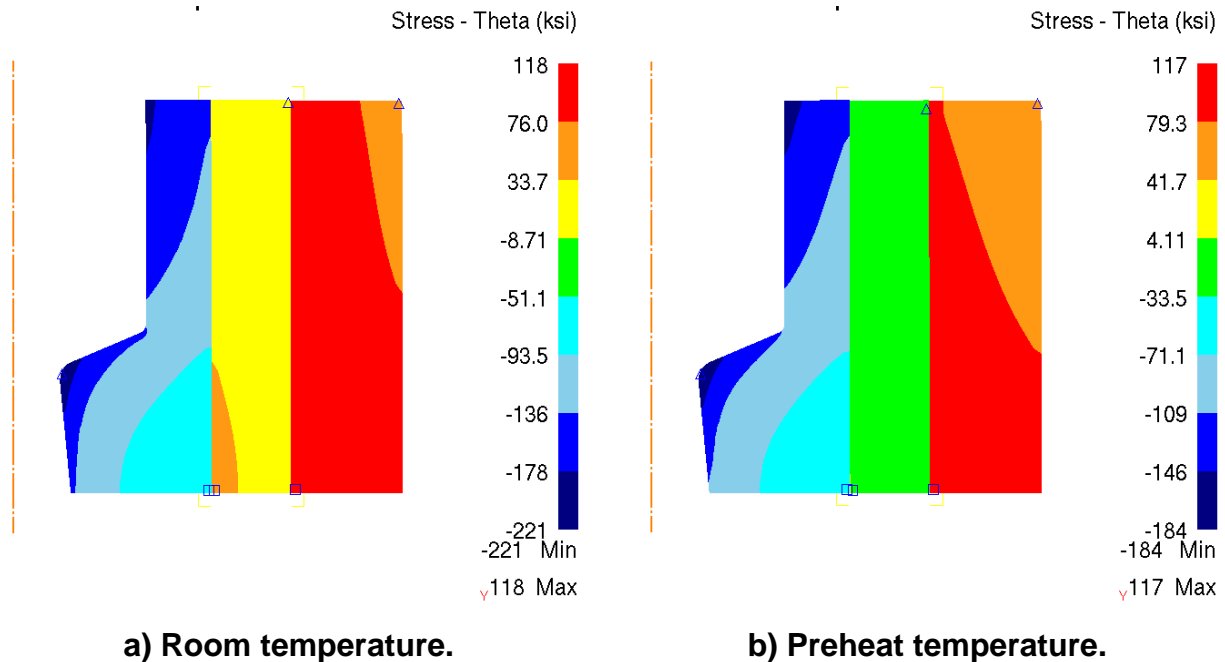


**Figure 17: Change in tangential pre-stress due to preheating for a die assembly with a ceramic insert.**

### 5.3.4 Die stresses at forging temperature and maximum load

During the forging process, the heat transfer between the workpiece and dies results in a localized increase in the surface temperature of the die insert. The expansion of the heated die surface is resisted by the cooler die substrate resulting in high compressive stresses in the surface of the die. Additionally, the die insert is also subjected to the mechanical loading during extrusion. In order to analyze this loading on the die insert, the following simulation procedure was used:

- Step 1: Import stress and elastic deformation history from the preheat die stress simulation (Section 5.3.3).
- Step 2: For the die insert, interpolate nodal forces from the workpiece onto the die surface in contact with the workpiece.
- Step 3: For the die insert, import the temperature distribution from the forging simulation for the step corresponding to the maximum forging load (breakthrough pressure).
- Step 4: Conduct a one-step die stress analysis.

Figure 18a shows the maximum principal stresses obtained from a conventional die stress analysis procedure. In this case, the shrink-fit values at room temperature are applied as boundary conditions on room temperature die geometries under hot forging temperature conditions. Thus, the stress and elastic deformation history from room temperature shrink-fitting and preheating (Sections 5.3.2 and 5.3.3) are neglected. Comparison of Figures 18a and 18b shows that the conventional approach underestimates the tensile stresses (especially in the die corner) by approximately 20-

25%. The compressive stresses on the other hand are overestimated by 15-90% depending upon the location. The stress distributions are also significantly different, except on the die shoulder which is governed mainly by thermal stresses. Thus, a conventional die stress analysis procedure would result in erroneous interpretation of the die design due to the assumptions that a) the shrink-fit values remain the same as those at room temperature (i.e. thermal expansion is negligible), and b) the shrink-fit interfaces and die assembly maintain the same dimensions as at room temperature (i.e. non-uniform elastic deflection of shrink fit interfaces is negligible).

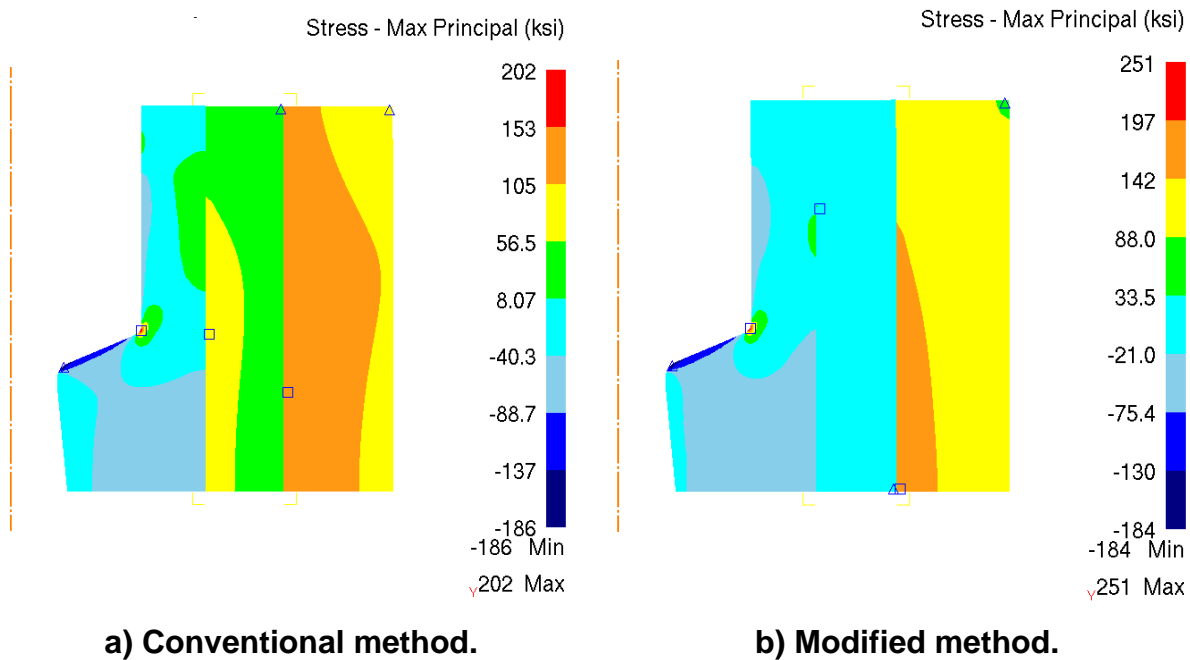


**Figure 18: Comparison of die stresses obtained using the conventional method and the modified method.**

The high local stress in the die corner occurs due to the selection of an insufficiently large radius. This can be remedied by increasing the radius and/or splitting the die insert into two pieces above the radius, either horizontally or axially. Such a split die design will also enable reduction of the high tensile stress in the outer ring.

### 5.3.5 Die stresses after part removal

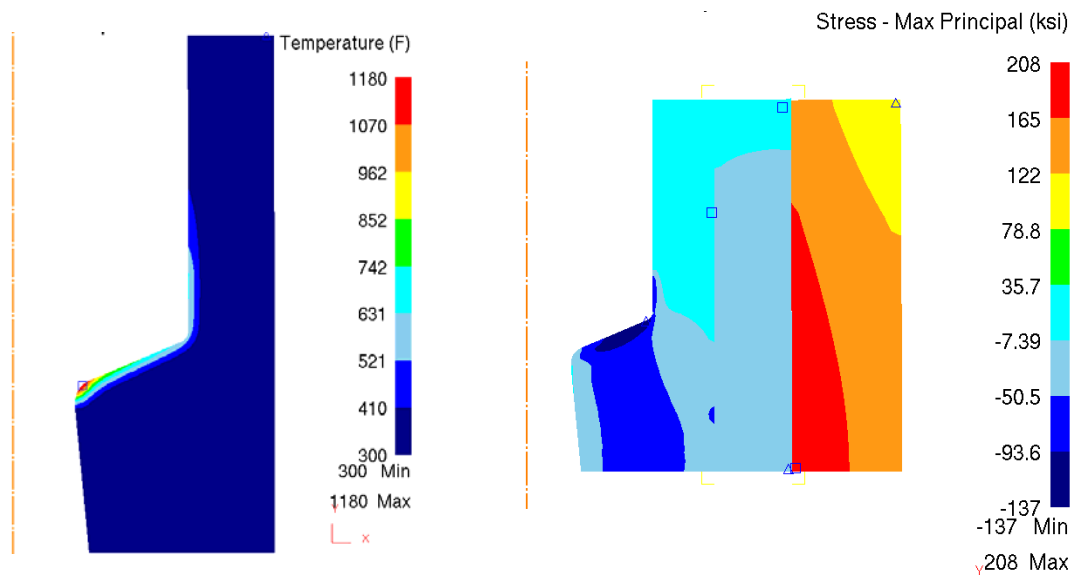
In the forging process, deformation is completed at bottom dead center (BDC) (time  $t_2$  in Figure 11). At this stage the punch starts to retract to TDC, but the part remains in the die insert until it is pushed out by the knockout pin. It was assumed that the knockout is done after the punch reaches TDC. During this time ( $t_2$  to  $t_c$  in Figure 11) there is heat transfer between the workpiece and the die insert. To determine the die stresses after part removal, the following two simulation stages were required.

#### 5.3.5.1 Stage 1: Die stresses at bottom dead center (BDC)

- Step 1: Import the stress and elastic deformation history from Section 5.3.4.

- Step 2: For the die insert import the temperature distribution from BDC of the forging simulation.
- Step 3: For the die insert interpolate the nodal forces from the workpiece, corresponding to the BDC position.
- Step 4: Conduct a one-step die stress analysis.

Stage 1 gives the temperature distribution and the stresses in the die assembly at BDC when the temperatures in the die reach a maximum (Figure 19). The high thermal gradient at the die surface again results in high compressive stresses on the die surface. However, these stresses are  $\approx 30\%$  lower compared to those that occur at maximum load (Section 5.3.4; Figure 19b), as the temperature gradient from the surface to the inside of the die is reduced due to the longer contact time. Thus, a die material with very good thermal conductivity will reduce the thermal stresses in the die surface layers. However, good tempering resistance is also required to prevent thermal softening and accelerated wear of the die surface.



a) Temperature in the die insert.

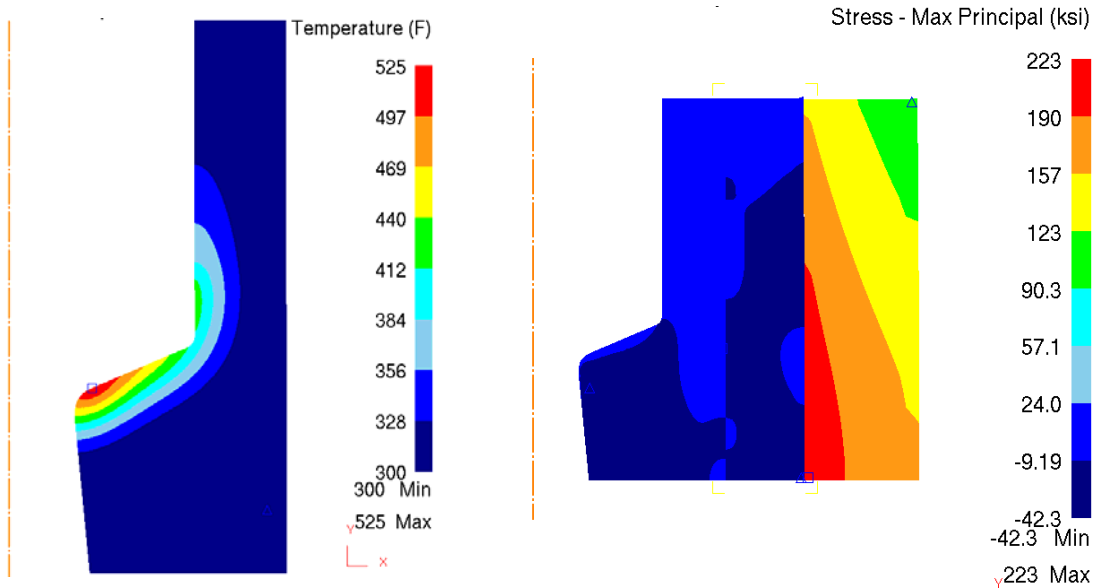
b) Maximum principal stress.

**Figure 19: Maximum principal stress and temperature distribution in the die at BDC.**

#### 5.3.5.2 Stage 2: Die stresses at the end of the forging cycle (at TDC)

- Step 1: Import the stress and elastic deformation history from the Stage 1 simulation of die stresses at BDC.
- Step 2: Import the temperature distribution at TDC from the forging simulation.
- Step 3: Conduct a one step die stress analysis.

Figure 20 shows the die stresses at the end of the press revolution when the punch has retracted back to TDC. During punch retraction ( $t_2$  to  $t_c$  in Figure 11), heat is conducted away by the underlying die substrate under near no-load conditions. The temperature gradient in the die drops, resulting in further reduction of surface compressive stress.



a) Temperature in the die insert.

b) Maximum principal stress.

**Figure 20: Maximum principal stress and temperature distribution at the end of the forging stroke (punch at TDC).**

### 5.3.6 Die stresses after lubricant spray

The die cooling phase consists of two separate stages, viz. the lubricant spray on the die surface and the dwell time between the end of spray and the start of the next forging cycle. The actual part knockout and removal time was not considered. It was assumed that the die is sprayed with the lubricant/cooling at the end of the forging cycle. However, these stages can be easily included in the process described below.

In order to simulate the lubricant/cooling spray the die insert surface is assigned an appropriately high interface heat transfer (IHT) coefficient corresponding to the lubrication spray settings. Numerous studies have been done using spray tests and FE simulation to correlate spray settings with interface heat transfer values (8;9). A value of 6164 Btu/hr-ft<sup>2</sup>-F (35 kW/m<sup>2</sup>-K) was used based on available literature, assuming the lubricant to be at room temperature (20°C/68°F). Similarly, the time between the end of lubricant spray and start of the next forging cycle is simulated by assigning the die surface an IHT coefficient of 4 Btu/hr-ft<sup>2</sup>-F (0.0227 kW/m<sup>2</sup>-K) corresponding to air at room temperature. These two simulations were carried out as follows:

- Step 1: Import the stress and elastic deformation history from the simulation of die stresses at TDC.
- Step 2: Assign a boundary condition on the inner die surface to simulate exposure to the lubricant spray.
- Step 3: Conduct a cooling simulation with the given boundary condition for the selected process duration (0.2 seconds).
- Step 4: Modify the boundary condition by changing the interface heat transfer coefficient on the die surface.

- Step 5: Conduct a subsequent dwell-time simulation for the selected process duration (0.2 seconds).

The stress state on the die surface after the cooling spray (Figure 21b) is reversed from those observed at BDC and TDC (Figures 19 and 20). The surface temperatures on the die shoulder drop from approximately 260°C (500°F) to 87°C (190°F) in the assumed spray duration of 0.2 seconds. The contraction of the die surface due to cooling is restricted by the hot die material beneath the surface layers resulting in tensile stresses. This repetitive thermal cycling results in heat checking on the die surface.

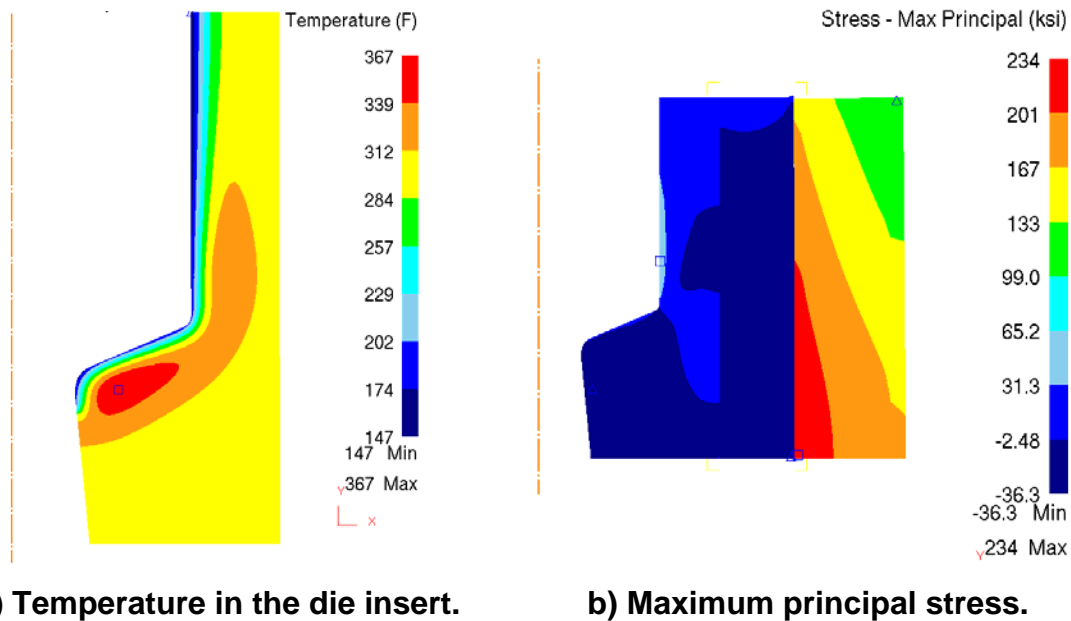
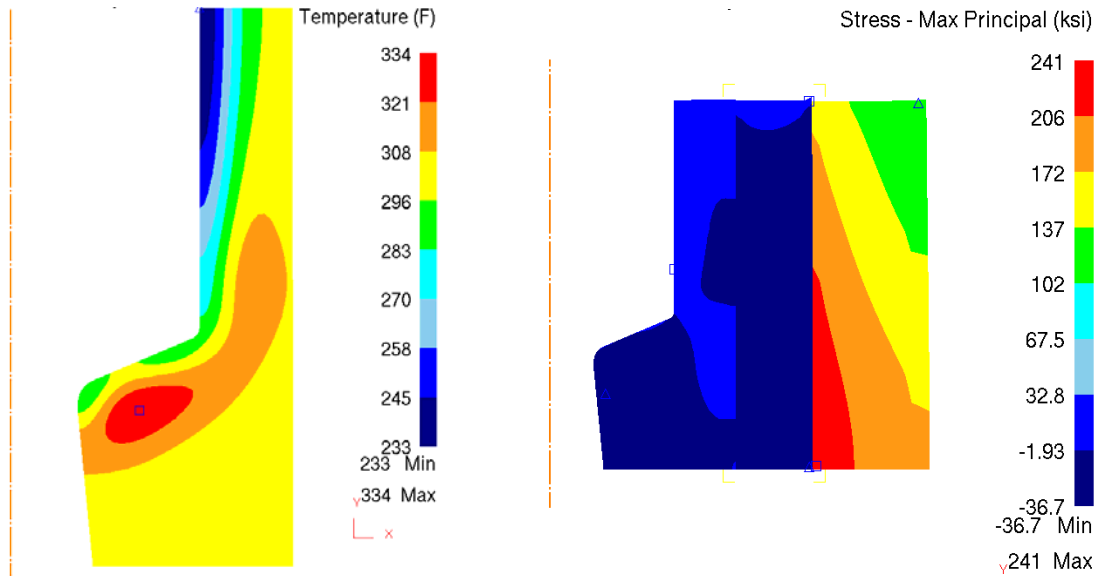


**Figure 21: Maximum principal stress and temperature distribution in the die after the lubricant/cooling spray.**

Figure 22 shows the temperature and stress distribution in the die prior to the next forging operation i.e. before the next billet is placed in the die. During the dwell period heat transfer occurs from the hot die substrate to the cooler surface layers resulting in an increase in the surface temperature, which now ranges between 110°C (230°F) to 148°C (300°F).

Figures 15 through 22 indicate that the outer ring is stressed close to its yield limit at the lower portion along with a stress concentration at the die corner. It should be noted that the die design considered was for purely demonstrative purposes and a realistic design might employ split-inserts with independent shrink-rings to reduce die stresses under load such as the schematic shown in Figure 23. Draft angles and tapers are not shown but would be required to lock the inserts and prevent any separation and flash formation.



a) Temperature in the die insert.

b) Maximum principal stress.

Figure 22: Maximum principal stress and temperature distribution in the die prior to the subsequent forging stroke.

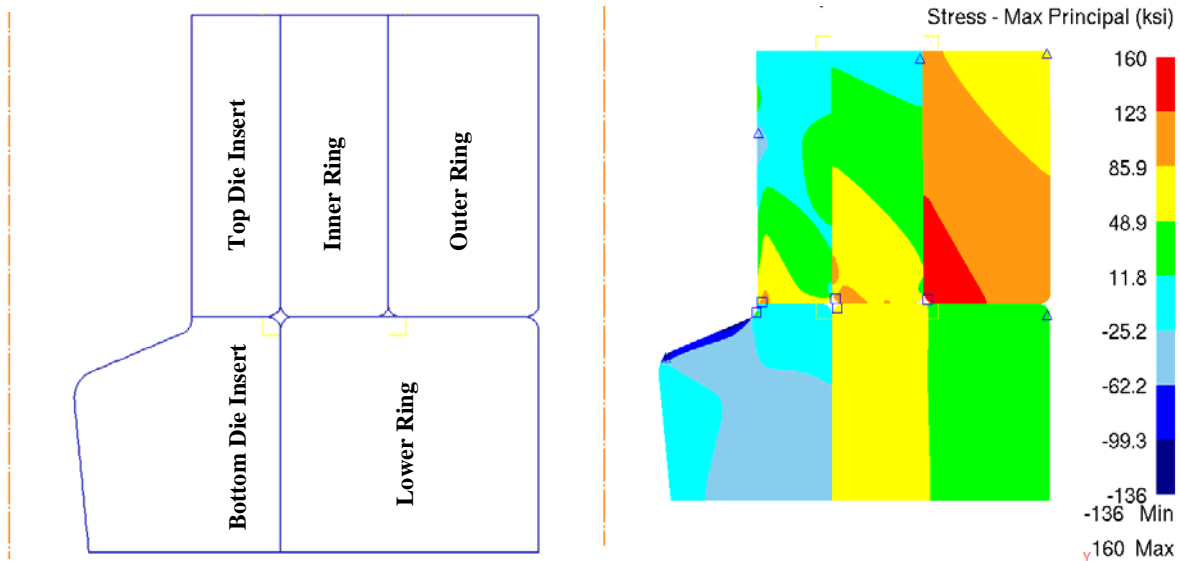


Figure 23: Schematic of a split-die design using two sets of shrink rings for reduction in die stresses at maximum load.

## 6 SUMMARY AND FUTURE OUTLOOK

The FIERF-sponsored die wear study being conducted at OSU aims to improve die life in hot and warm forging die applications through the application of die materials such as new proprietary hot-work steel grades and advanced ceramics. This study is being conducted in active cooperation with forge shops, lubricant suppliers and tooling



companies. The project officially commenced on July 15, 2006 with a proposed duration of 12 months. The current status of the project is as follows:

- A consortium of FIA member companies has been formed in order to select example parts with die life related problems. Tooling companies and lubricant suppliers are also a part of this working group.
- An extensive global literature review was conducted on die wear related studies and summarized in the form of two literature review reports available to the participating companies.
- An axisymmetric hot forged part was selected for initial forging trials. Based on detailed FE analysis of the die-workpiece interface conditions, die design modifications were suggested in the buster and finisher stage to reduce contact time during forging. An advanced hot-work tool steel Uddeholm W360™ will be used for the first forging trials tentatively planned for March 2007.
- A hypothetical warm forward extrusion process was considered to demonstrate the importance of preheat temperature and forging temperature gradients on a shrink-fit tool design. Conventionally, room temperature shrink-fit values and die geometries are used for design and analysis of hot and warm forging die assemblies. This can lead to significant errors especially when the thermal expansion coefficient of the insert material is significantly less than that of the shrink rings as is the case with ceramics. In the current study, it was found that the results with the conventional method show significant errors even when a hot-work tool steel insert was considered. Thus, the elastic deflection and stress history from the room temperature die assembly and preheating should be accounted for in design shrink-fit tooling for hot and warm forging processes.

Based upon the results of the preliminary forging trials, further studies will be conducted with more complicated geometries from the viewpoint of developing die designs for improved die life along with the application of advanced die materials. For further information on this study please visit [www.ercnsm.org](http://www.ercnsm.org) or contact Dr. Taylan Altan at [altan.1@osu.edu](mailto:altan.1@osu.edu).

## References

1. Behrens, B.A., Barnert, L., and Huskic, A., "Alternative Techniques to Reduce Die Wear – Hard Coating or Ceramic?", Annals of the German Academic Society for Production Engineering (WGP), 2005.
2. Mitamura, K., and Fujikawa, S., "Application of Boride Cermet in Warm Forging Dies", (Nissan Mortor Co., Ltd.).
3. Iwase, S., Yoshizaka, M., Yamada, S., and Fujimoto, H., "Hot forging of Ti alloy valve preforms", Aisan Kogyo Kabushiki Kaisha, Obu, Japan, US Patent # 5964120, October 1999.
4. Horie, N., Sato, K., Kanda, Y., Mitamura, K., Hamazaki, K., and Kori, T., "Cermet hot forging die", Asahi Glass Company, Tokyo, Japan, US Patent # 5406825, April 1995.
5. ICFG Data Sheet No. 6/72, "Dies (Die Assemblies) for Cold Extrusion of Steel", prepared by the International Cold Forging Group, sponsored, OECD, and published in English on their behalf by the Institute of Sheet Metal Engineering.
6. "Source Book on Cold Forming", American Society for Metals (ASM), June 1975.
7. Lange, K., "Handbook of Metal Forming", Society of Manufacturing Engineers, ISBN 0-87263-457-4, 1985.
8. Sawamura, M., Yogo, Y., Kondo, S., Tanaka, T., Nakanishi, K., Suzuki, T., and Watanabe, A., "Estimation of Spray Lubrication and Die Temperature for Die Wear Life Prediction in Hot Forging", R & D Review of Toyota CRDL, Vol. 40, No. 1, 2005.
9. Tanaka, T., Nakanishi, K., Yogo, Y., Kondo, S., Tsuchiya, Y., Suzuki, T., and Watanabe, A., "Prediction of Hot Forging Die Life Using Wear and Cooling Model", R & D Review of Toyota CRDL, Vol. 40, 2005, No. 1.